Supplementary Figure 1

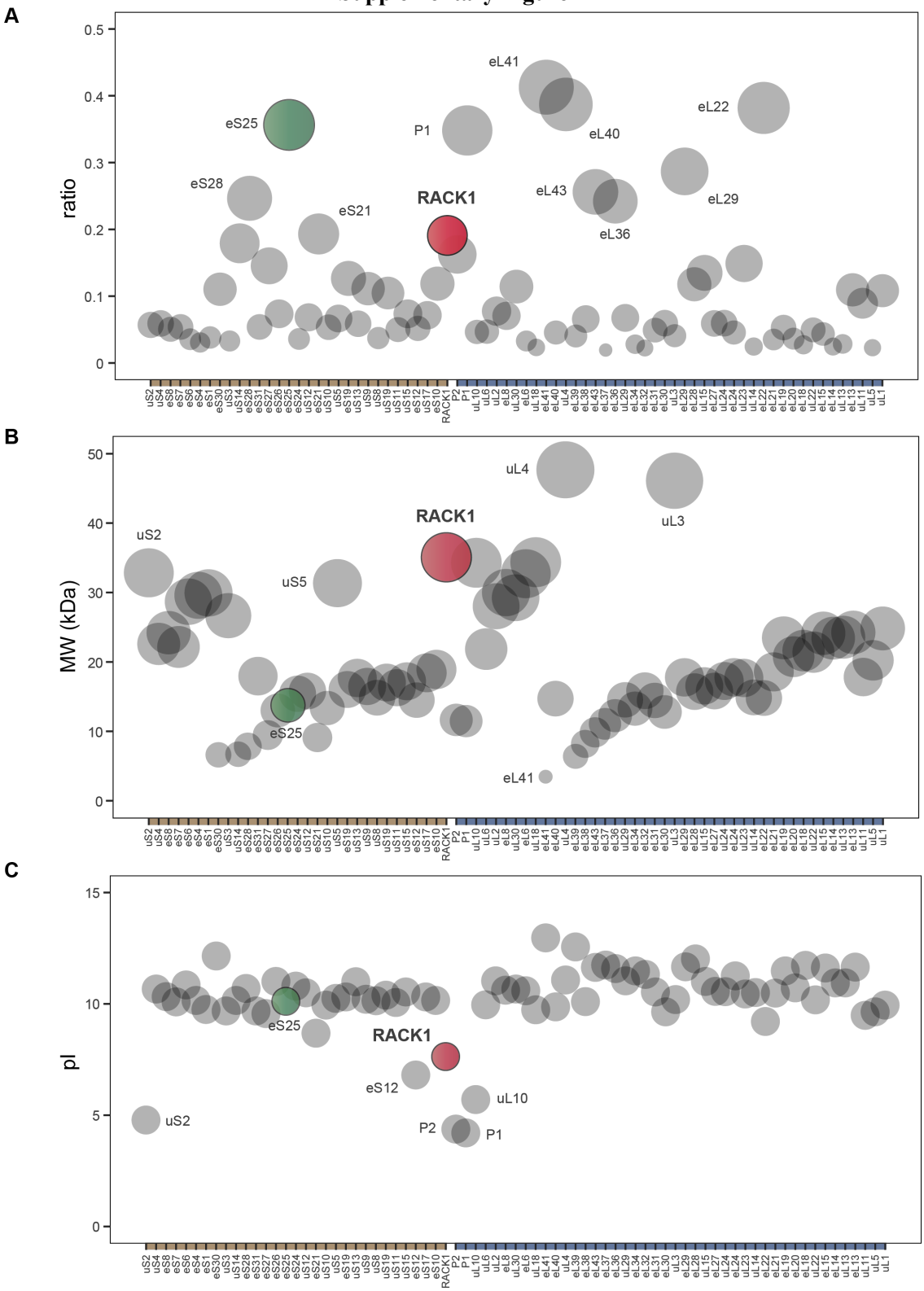

Supplementary Figure 1. Properties of human ribosomal proteins. For all plots, the small subunit ribosomal proteins are plotted on the left, while those of the large subunit are on the right (tan and blue regions of x-axis, respectively). Proteins are annotated with the new nomenclature for ribosomal proteins, and ribosomal protein paralogs were omitted in this analysis. RACK1 is indicated in red and eS25 is indicated in green. For a and b, the size of each plotted circle reflects the magnitude of the y-axis value.

A. Ratio of sense to antisense gene-trap insertions from essentiality screen in HAP1 cells (Blomen et al. 2015). While the absolute number of insertions can limit confidence in assigning essential genes, this metric allows an approximation for RP genes that may be deleted without substantial fitness costs (higher ratio ~ less essential). This is supported by our ability to generate isogenic knockouts of RPS25 and RACK1, but the essentiality of several of the other high ratio genes have yet to be rigorously analyzed in human cells.

B. Size distribution of human ribosomal proteins based on their predicted molecular weight (MW) in Daltons (Da).

C. Isoelectric point (pI) distribution of human ribosomal proteins. For b and c, protein statistics were retrieved from Uniprot.

Supplementary Figure 2

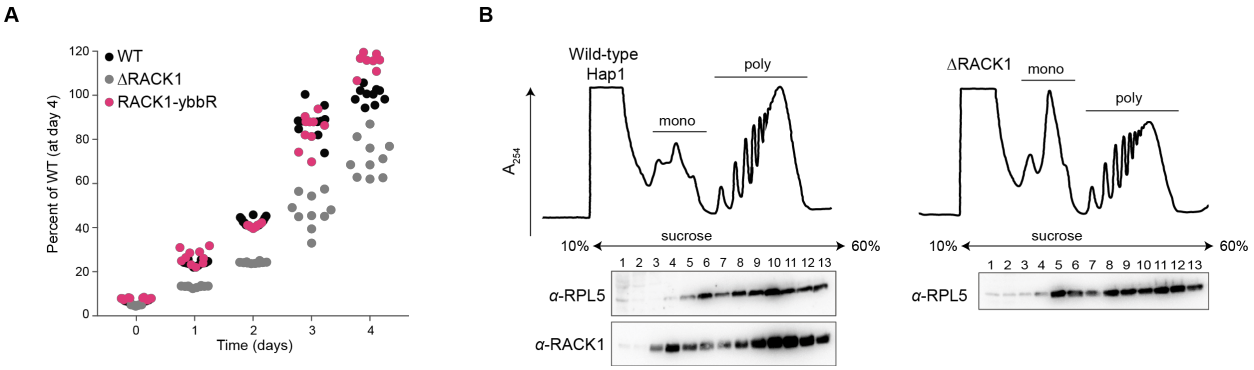

Supplementary Figure 2 (related to Figure 1). RACK1-ybbR incorporates into translating ribosomes in cells.

A. Plot of the proliferation of the indicated cell lines as measured by MTT assay relative to the wild-type cells at day 4. Each circle represents cells from a distinct well in a 96-well plate, and these data were used to generate the line graph in Figure 1b.

B. UV absorbance traces (at 254 nm) of polysome profiling and associated western blot analyses. "Mono" and "poly" refer to peaks that correspond to monosomes and polysomes, respectively.

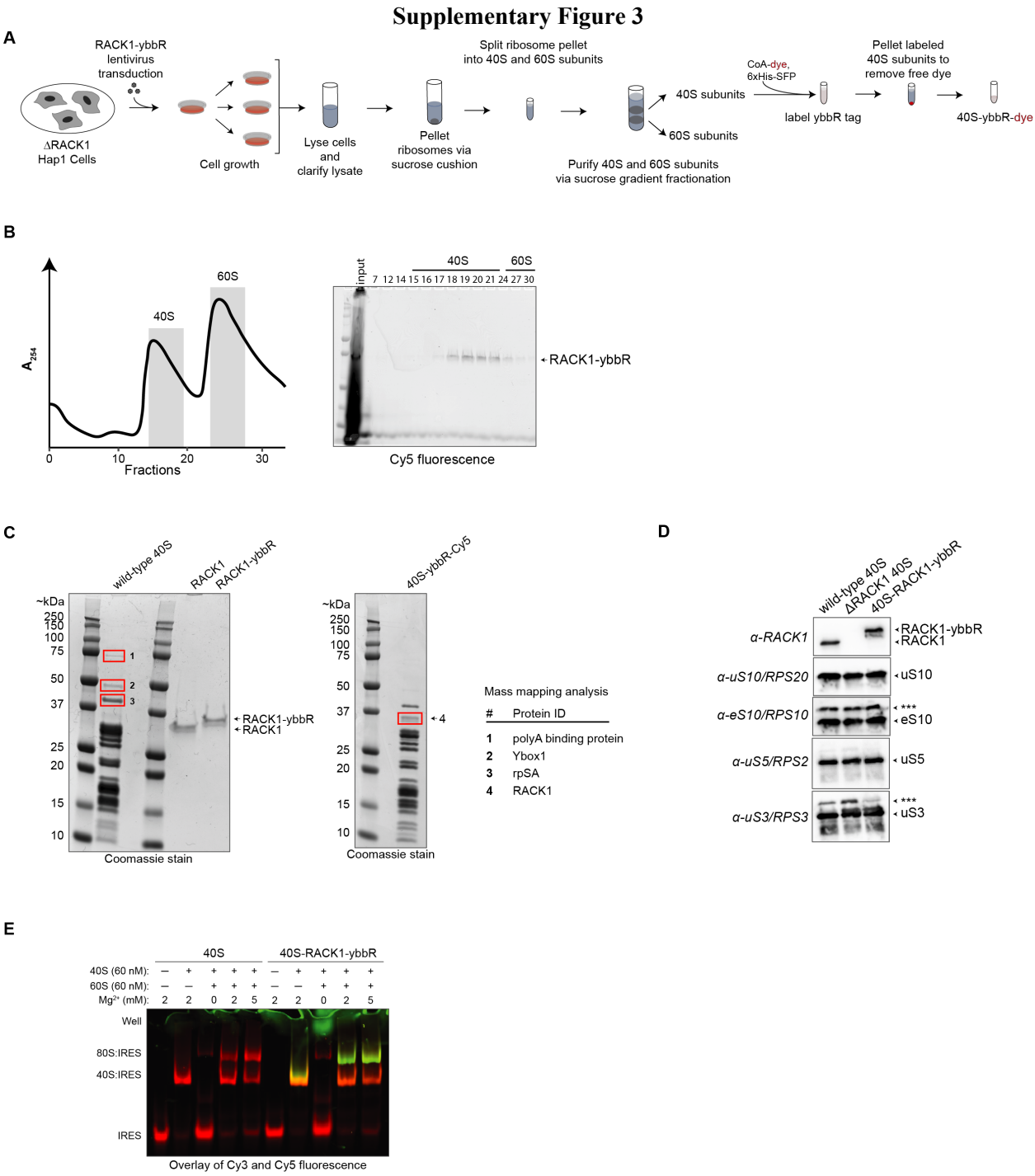

Supplementary Figure 3 (related to Figure 2). Purification and biochemical characterization of ribosomes labeled with RACK1-ybbR.

A. Strategy to purify and fluorescently label ribosomal subunits from the human HAP1 cell line.

B. A representative UV absorbance trace (at 254 nm) (left) and an image of a gel scanned for Cy5 fluorescence (right) following SDS-PAGE analysis of the sucrose gradient fractionation step from our initial attempt to fluorescently-label 40S-RACK1-ybbR subunits. Crude 80S ribosomes (after the first

sucrose cushion) from RACK1-ybbR expressing cells were resuspended in a standard high-salt and puromycin-containing subunit splitting buffer supplemented with 10 mM Mg^{2+}. After incubation with SFP synthase and CoA-Cy5, we quenched the excess magnesium, split the ribosomes into individual subunits, and purified them using a 10-30% sucrose gradient followed by fractionation, with each fraction examined for Cy5 fluorescence using SDS-PAGE. The single band of Cy5 fluorescence matched the molecular weight of RACK1-ybbR and was primarily localized to the 40S ribosomal subunit peak. Despite its initial promise, however, these ribosomes were poorly labeled, which we attributed to the high concentration of monovalent salt and other contaminants present in the crude 80S ribosomes during labeling. Nevertheless, the trace represents the typical separation of 40S and 60S ribosomal subunits by sucrose gradient fractionation, with the gray bars representing the portions of the peaks that were collected.

C. SDS-PAGE analysis of wild-type 40S ribosomal subunits, 40S ribosomal subunits labeled with Cy5 via RACK1-ybbR (40S-ybbR-Cy5), as well as recombinant wild-type RACK1 and RACK1-ybbR. The bands highlighted in red boxes correspond to the proteins identified by mass mapping analysis in panel e.

D. Western-blot analyses of the indicated purified 40S ribosomal subunits with select antibodies targeting proteins know to be involved in regulatory ribosomal protein ubiquitination. Asterix (***) indicate higher MW protein species, likely due to ribosomal protein modifications. The faint band below the RACK1-ybbR band may be due to partial cleavage of the ybbR tag, which is not labeled by SFP synthase.

E. Native gel electrophoresis analysis of wild-type or 40S-RACK1-ybbR-Cy3 for binding to the HCV IRES (Cy5), and forming 40S-IRES and 80S-IRES complexes. Complexes were formed with the indicated ribosomal subunits at 2-fold excess to the HCV IRES, and the indicated Mg^{2+} concentration.

Supplementary Figure 4

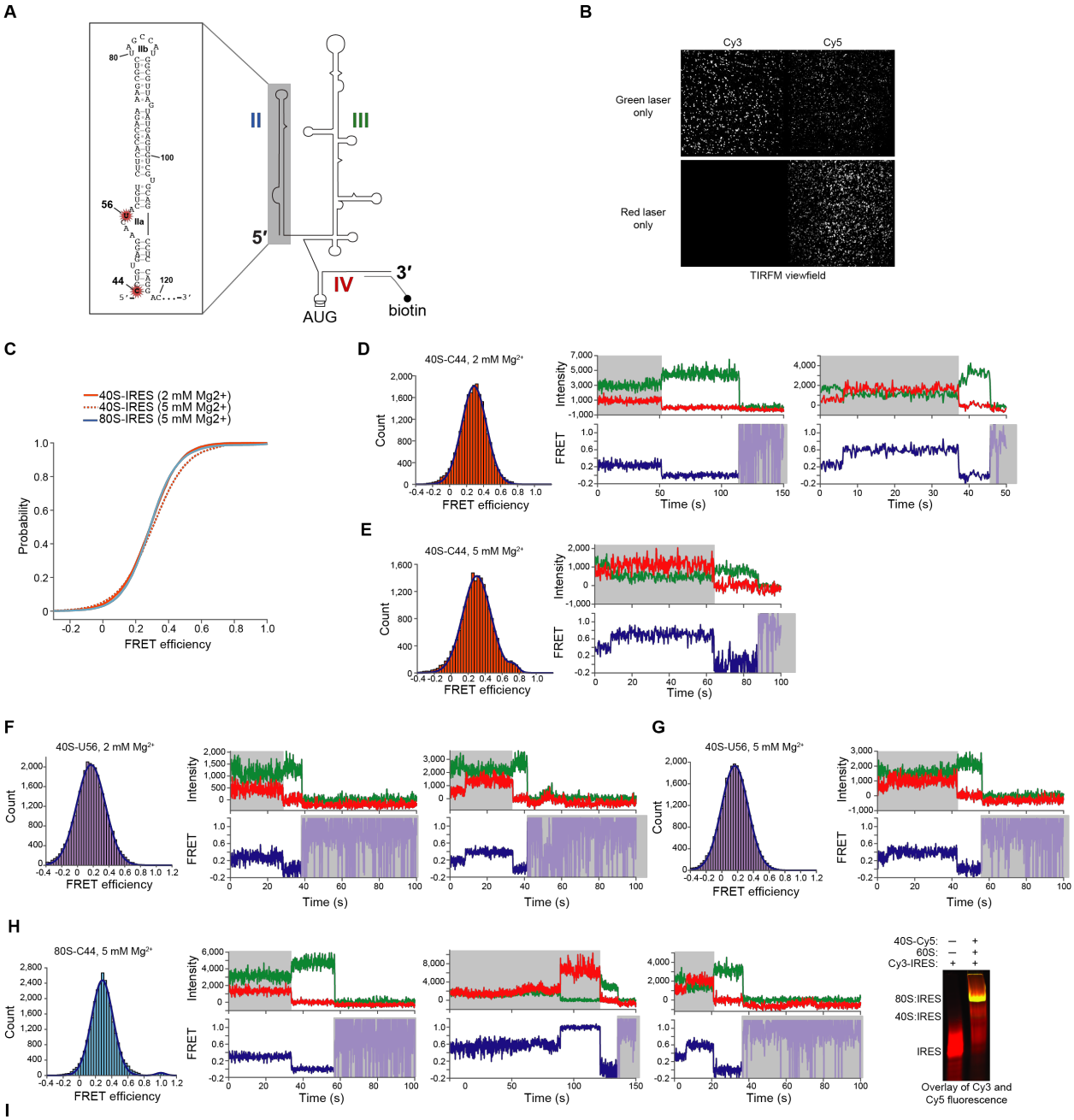

I

IRES label	Ribosome	[Mg2+] (mM)	Measured distance (Å)	Predicted FRET efficiency	Gaussian	A_1	95% CI	A_2	95% CI	Mean 1 (M_1)	95% CI	Mean 2 (M_2)	95% CI	Std. Dev. 1 (S_1)	95% CI	Std. Dev. 2 (S_2)	95% CI	Adj. R^2	n
Cy5-C44	40S-RACK1-Cy3	2	70	0.174	single	1807	28	NA	NA	0.28	0.002	NA	NA	0.20	0.003	NA	NA	0.99	107
Cy5-C44	40S-RACK1-Cy3	5	70	0.174	single	1420	30	NA	NA	0.30	0.004	NA	NA	0.23	0.005	NA	NA	0.99	101
					double	1429	25	98	43	0.30	0.003	0.73	0.02	0.23	0.005	0.076	0.04	0.99	101
Cy5-C44	40S-reconRACK1-Cy3	2	70	0.174	single	2117	54	NA	NA	0.31	0.006	NA	NA	0.29	0.008	NA	NA	0.98	100
Cy5-C44	40S-reconAsc1p-Cy3	2	70	0.174	single	939	17	NA	NA	0.33	0.003	NA	NA	0.25	0.005	NA	NA	0.99	106
					double	939	17	29	31	0.33	0.003	1.0	0.06	0.25	0.005	0.072	0.08	0.99	106
Cy5-C44	80S-RACK1-Cy3	5	70	0.174	single	2475	54	NA	NA	0.28	0.003	NA	NA	0.18	0.004	NA	NA	0.99	277
					double	2475	53	68	79	0.28	0.003	1.0	0.07	0.18	0.004	0.083	0.1	0.99	277
Cy5-U56	40S-RACK1-Cy3	2	90	0.045	single	2043	30	NA	NA	0.17	0.003	NA	NA	0.25	0.004	NA	NA	0.99	141
Cy5-U56	40S-RACK1-Cy3	5	90	0.045	single	1933	23	NA	NA	0.16	0.002	NA	NA	0.24	0.003	NA	NA	0.99	137

Single gaussian: $f(x) = A_1 * \exp(-((x-M_1)/S_1)^2)$

Double gaussian: $f(x) = A_1 * \exp(-((x-M_1)/S_1)^2) + A_2 * \exp(-((x-M_2)/S_2)^2)$

Supplementary Figure 4 (related to Figure 3). RACK1-ybbR is proximal to domain II of the HCV IRES and provides a signal for 40S-IRES conformational dynamics.

A. Schematic of the secondary structure of the HCV IRES indicating domains II, III, and IV. Inset box shows an expansion of domain II with secondary structure of nucleotides, indicating positions of fluorescent labels at C44 and U56. An extension at the very 3' end of the HCV IRES RNA was used to anneal a biotinylated oligo for immobilization in all single-molecule experiments.

B. Example view field from TIRFM analyses of the 40S-RACK1-ybbR-Cy3:Cy5-IRES(C44) complex.

C. Cumulative distribution plot of observed FRET intensities for RACK1-ybbR-Cy3 bound to IRES(Cy5-C44) (purple) either in a 40S-IRES complex in the presence of 2 mM Mg^{2+} (solid orange line) or 5 mM Mg^{2+} (orange dotted line), or in an 80S-IRES complex (solid blue line).

D. FRET intensity histogram for 40S-RACK1-ybbR-Cy3 FRET with IRES(Cy3-C44) at 2 mM Mg^{2+} and representative single-molecule fluorescence traces. FRET intensity data were fit with a single Gaussian distribution.

E. FRET intensity histogram for 40S-RACK1-ybbR-Cy3 FRET with IRES(Cy3-C44) at 5 mM Mg^{2+} and a representative single-molecule fluorescence trace. FRET intensity data was fit with a double Gaussian distribution.

F. FRET intensity histogram for 40S-RACK1-ybbR-Cy3 FRET with IRES(Cy3-U56) at 2 mM Mg^{2+} and representative single-molecule fluorescence traces. FRET intensity data were fit with a single Gaussian distribution.

G. FRET intensity histogram for 40S-RACK1-ybbR-Cy3 FRET with IRES(Cy3-U56) at 5 mM Mg^{2+} and representative single-molecule fluorescence traces. FRET intensity data were fit with a single Gaussian distribution.

H. FRET intensity histogram for 80S-RACK1-ybbR-Cy3 FRET with IRES(Cy3-C44) at 5 mM Mg^{2+} and representative single-molecule fluorescence traces. FRET intensity data were fit with a double Gaussian distribution. After collecting TIRFM data, excess complex was analyzed by native gel electrophoresis to verify successful 80S formation (gel on right). Cy3 and Cy5 overlay used to indicate major co-localized fluorescent species.

I. Table of parameters yielded from fitting the indicated experiments to single or double Gaussian distributions. Also showing distance measurements between labeling positions using PDB 5a2q and predicted FRET efficiencies for the Cy3-Cy5 dye pair.

Supplementary Figure 5

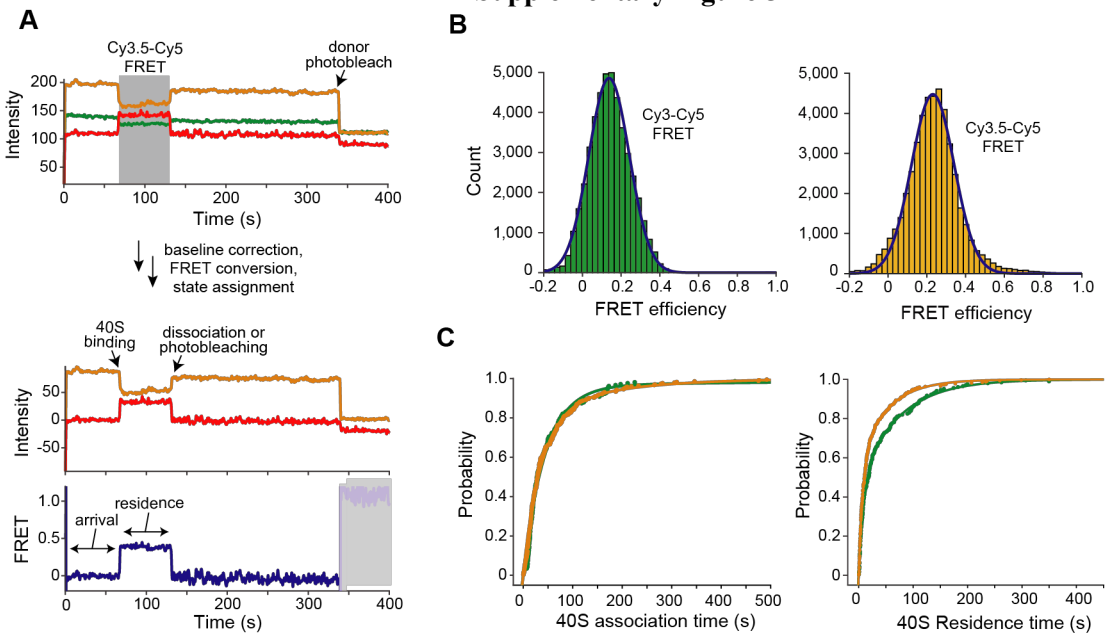

D

IRES label	R0 (Å/J(λ) in cm3 M−1)	Measured distance (Å)	Predicted FRET efficiency	Amp. (A)	95% CI	Mean (M)	95% CI	Std. Dev. (S)	95% CI	Adj. R^2	n
Cy3	54/9.37e−13	70	0.17	4856	91	0.13	0.002	0.14	0.003	0.99	175
Cy3.5	60/1.69e−12	70	0.28	4476	121	0.23	0.003	0.15	0.004	0.99	194

$f(x) = A*\exp(-((x-M)/S)^2)$

E

Fit	IRES label	A_{fast}	95% CI	k_{fast}	95% CI	k_{slow}	95% CI	Adj. R^2	n
Association	Cy3	0.96	0.04	0.022	0.001	0.0010	0.005	0.97	175
Association	Cy3.5	0.81	0.08	0.027	0.002	0.0062	0.002	0.99	194
Residence	Cy3	0.45	0.01	0.11	0.006	0.014	0.0006	0.99	175
Residence	Cy3.5	0.58	0.02	0.12	0.005	0.019	0.001	0.99	194

$f(x) = A_{fast}*(1-\exp(-k_{fast}*x))+(1-A_{fast})*(1-\exp(-k_{slow}*x)) + d$

Supplementary Figure 5 (related to Figure 3). Monitoring 40S-IRES association kinetics by real-time smFRET in ZMWs.

A. Example single-molecule fluorescence trace that depicts Cy3.5-Cy5 FRET upon delivery of 40S-RACK1-ybbR-Cy5 to dual-immobilized IRES(Cy3-C44) and IRES(Cy3.5-C44). The trace is displayed as in Figure 4b, and schematic used to show the process for extracting FRET efficiency and kinetic parameters. Briefly, ZMWs with either a single Cy3- or Cy3.5-IRES(C44) molecule were identified by a single-step photobleaching event of the donor fluorophore, based on their relative intensities. The respective FRET events are highlighted in grey, and photobleaching of the donors are indicated by the arrows. After selecting single molecules for each dye pair, we corrected for background fluorescence in each optical channel and calculated distributions of observed smFRET efficiencies for the Cy3-Cy5 and Cy3.5-Cy5 dye pairs.

B. FRET intensity histograms for IRES(Cy3-C44, left green bars) or IRES(Cy3.5-C44, right orange bars) with 40S-RACK1-ybbR-Cy5. FRET intensity data were fit with single Gaussian distributions. Data is as in Figure 4c, but the histograms are now separated for clarity.

C. Cumulative distribution plot of observed 40S association and residence times upon delivery to dual-immobilized IRESs. Colors reflect the separate Cy3 and Cy3.5 IRES data as in Figure 3. The lines

represent fits to double-exponential functions with all fitting parameters in panel e. Given that the residence time of the 40S ribosomal subunit is concentration-independent, we attributed the minor difference in observed residence times with the two smFRET pairs to their distinct photophysical properties.

D. Table of parameters yielded from fitting the indicated experiments to single or double Gaussian distributions. Also showing distance measurements between labeling positions using PDB 5a2q and predicted FRET efficiencies for the Cy3-Cy5 and Cy3.5-Cy5 dye pairs.

E. Table of parameters yielded from fitting the indicated experiments to double-exponential functions.

Supplementary Figure 6

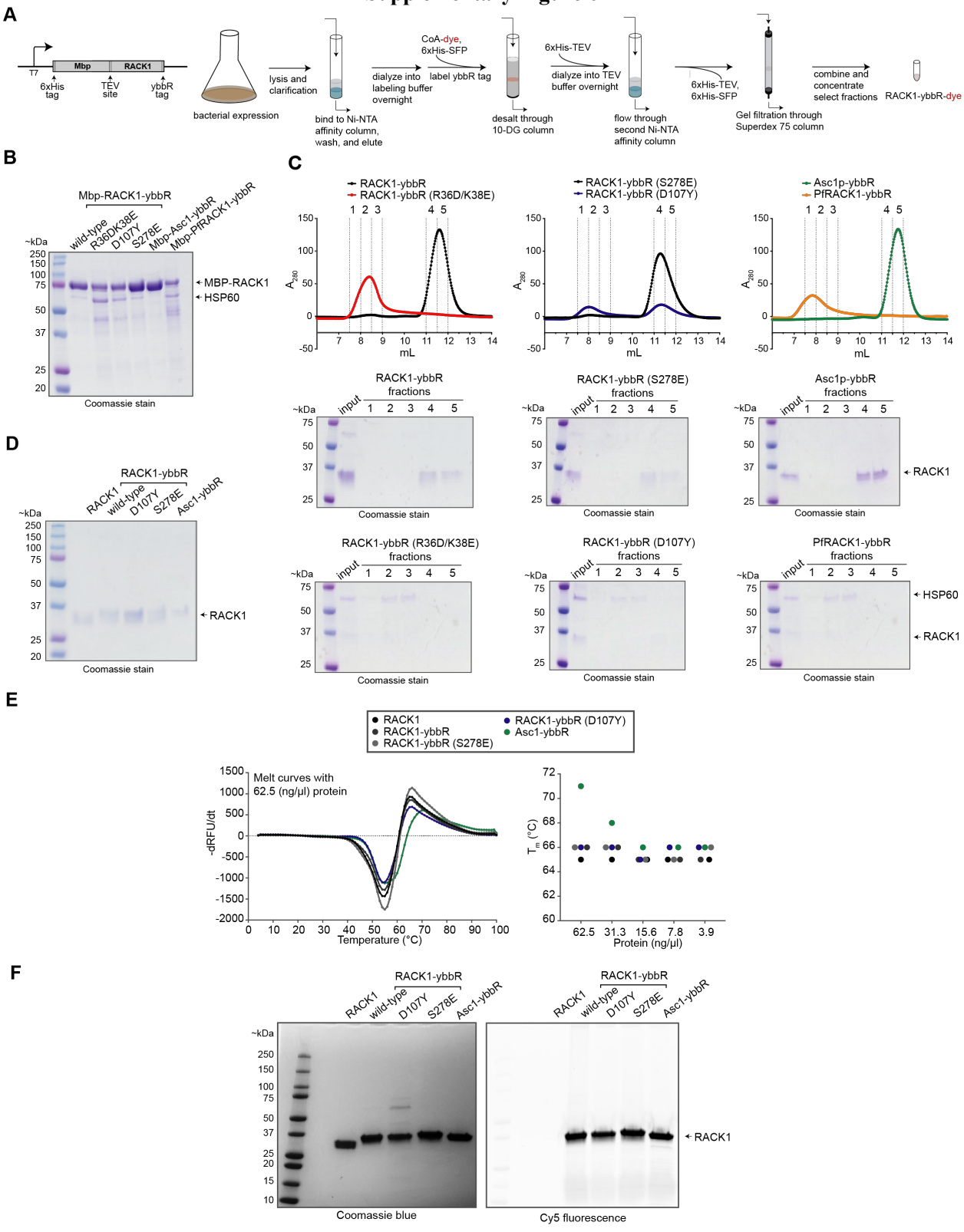

Supplementary Figure 6 (related to Figure 4). Purification and biochemical characterization of ybbR-tagged RACK1 mutants and homologs.

A. Strategy to purify and fluorescently label recombinant RACK1-ybbR proteins.

B. SDS-PAGE analysis of unlabeled 6xHis-Mbp-RACK1-ybbR proteins following first Ni-NTA purification and before TEV cleavage to remove MBP tag.

C. Gel filtration profiles (Superdex 75) of unlabeled and ybbR-tagged RACK1 proteins following TEV cleavage and removal of tag by second Ni-NTA column. SDS-PAGE analysis of select fractions shows the presence of HSP60-bound RACK1 proteins in the void volume for select mutants (R36D/K38E and D107Y) and homologs (*Plasmodium falciparum* PfRACK1), while monomeric RACK1 elutes at ~11 mL.

D. SDS-PAGE of purified and unlabeled RACK1 proteins after concentration of fractions that elute at 11-12 mL for each protein.

E. Thermal melt curves of various RACK1 proteins. The left panel shows the derivative of the relative fluorescence units (RFU) for melting of all proteins at 62.5 ng/µL. The right panel shows the estimated melting temperature (T_m) for each protein at five concentrations.

F. SDS-PAGE analysis of purified, concentrated, and Cy5-labeled RACK1-ybbR proteins. Both images are of the same gel, which was first scanned for Cy5 fluorescence (right) and subsequently stained with Coomassie blue (left). The band at ~60kD in the D107Y mutant corresponds to HSP60.

Supplementary Figure 7

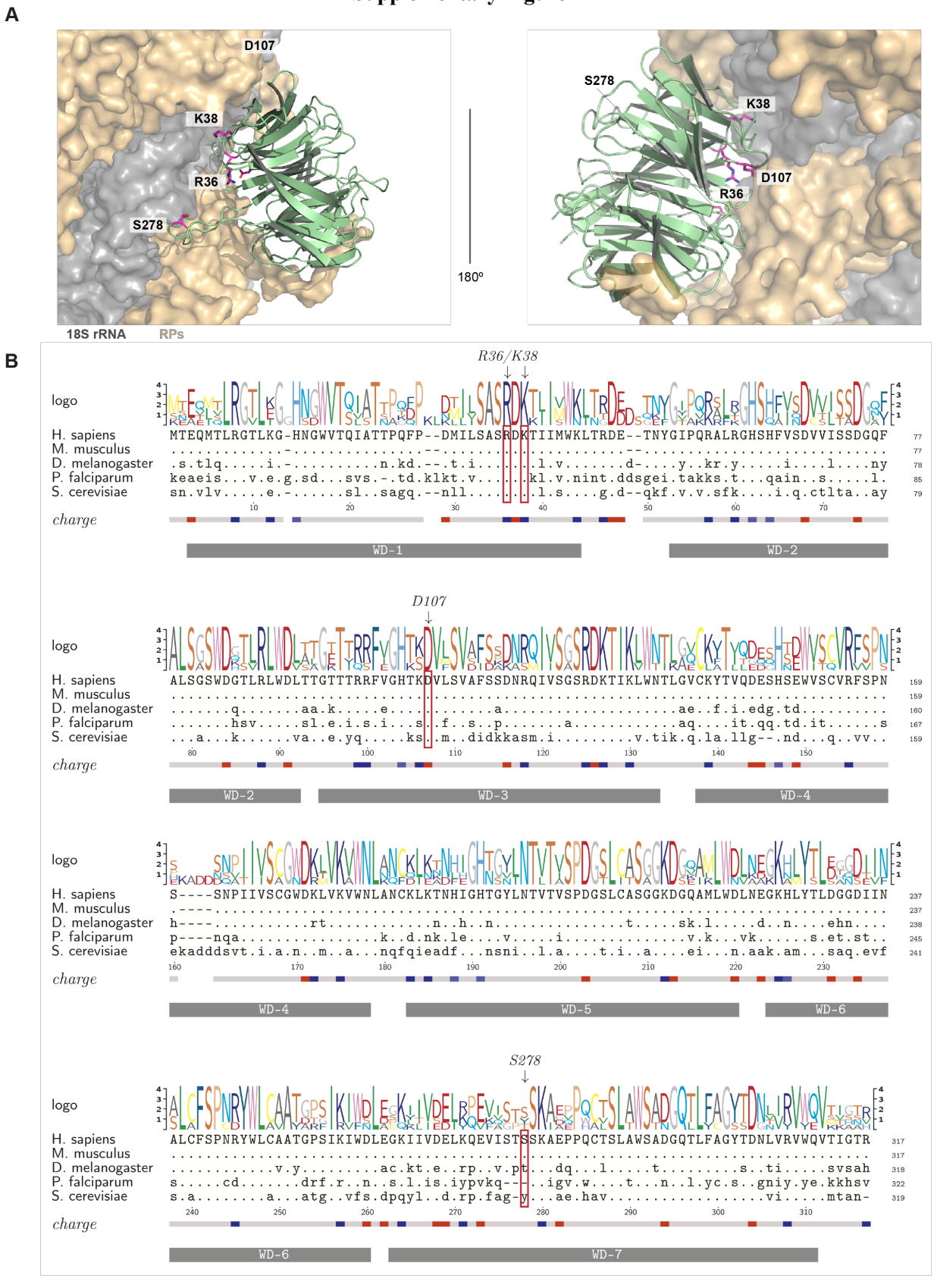

Supplementary Figure 7 (related to Figure 4). Location and conservation of RACK1 and its mutants.

A. Model structure of RACK1 bound to the 40S ribosomal subunit (PDB: 5a2q), with the substituted residues indicated. The 18S rRNA is in grey, and ribosomal proteins are in tan.

B. Alignment of the protein sequences for the indicated RACK1 orthologs. The residues boxed with red frames are those that are indicated in panel a.

Supplementary Figure 8

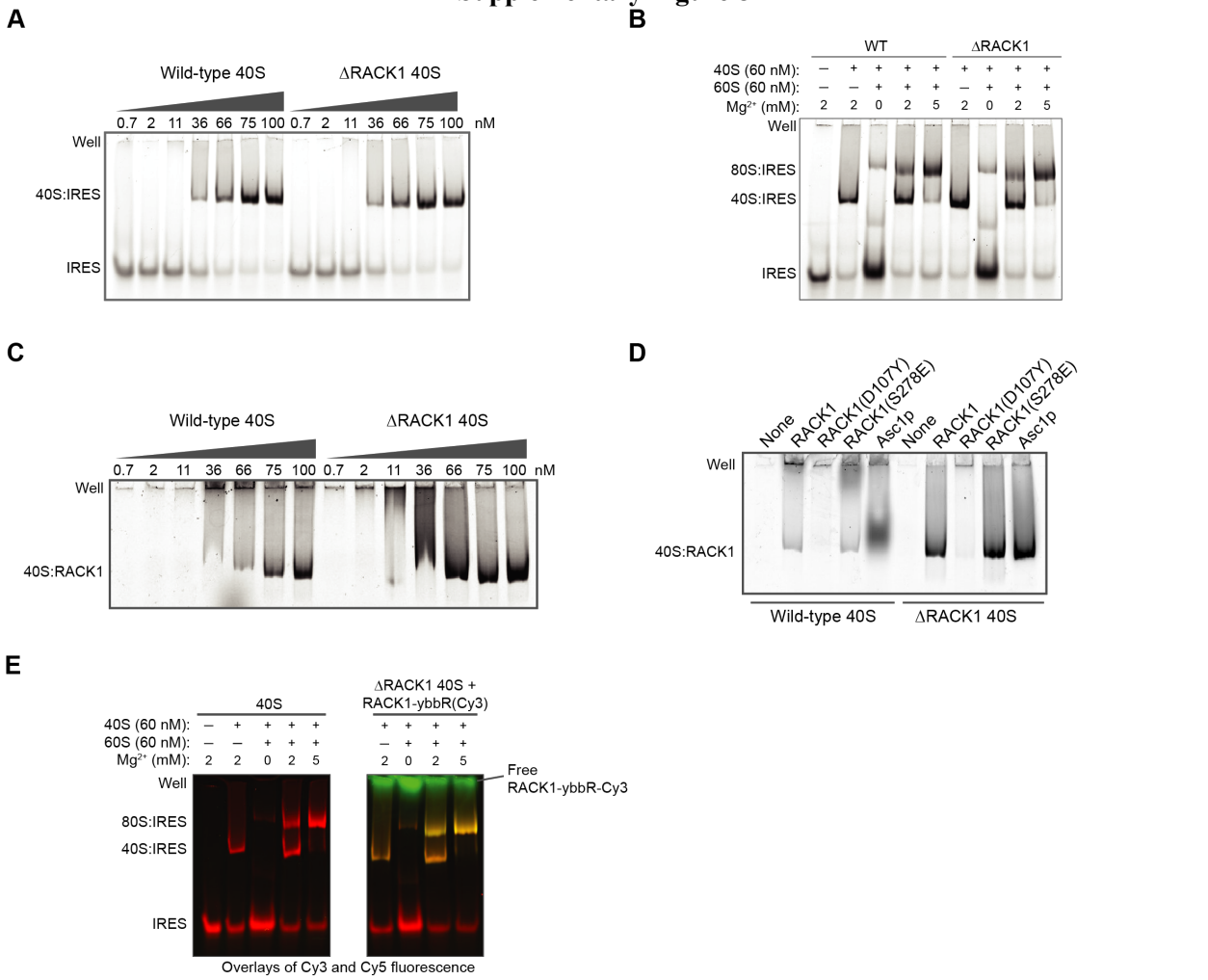

Supplementary Figure 8 (related to Figure 4). *In vitro* reconstitution of RACK1 to study RACK1 association with human ribosomes.

A. Native gel analysis of the indicated 40S ribosomal subunits binding to Cy5-labeled HCV IRES.

B. Native gel analysis of wild-type and ΔRACK1 ribosomes forming 40S- and 80S-IRES complex on a Cy5-labeled HCV IRES.

C. Native gel analysis of recombinant RACK1-ybbR-Cy5 incorporation into the indicated 40S ribosomal subunits. The concentration of RACK1-ybbR-Cy5 was 40 nM, and the concentration of 40S subunits are indicated above each lane. A representative gel is shown.

D. Native gel analysis of recombinant RACK1-ybbR-Cy5, RACK1(D107Y)-ybbR-Cy5, RACK1(S278E)-ybbR-Cy5, and Asc1p-ybbR-Cy5 incorporation into the indicated 40S ribosomal subunits (75 nM). The concentration of each protein was 40 nM.

E. Native gel analysis of reconstituted 80S ribosomes binding to Cy5-labeled HCV IRES. Wild-type 40S and in vitro reconstituted ΔRACK1 40S:RACK1-ybbR-Cy3 were analyzed in parallel. The gel displays the overlay of Cy3 (green) and Cy5 (red) fluorescence signals.

F. Cumulative distribution plot and histograms for FRET efficiency for reconstituted RACK1-ybbR-Cy3 ("RACK1 recon") and Asc1p-ybbR-Cy3 ("Asc1p recon") ribosomes versus the natively-purified 40S-RACK1-ybbR ribosomes. FRET intensity histograms show counts for the RACK1 and Asc1p reconstituted ribosomes on the left (blue) and right (green), respectively. The number of traces analyzed are indicated in Supplemental Figure 4i.

G. Example single-molecule fluorescence traces that captured FRET between the indicated 40S ribosomal subunits labeled with Cy3 and HCV IRES(C44-Cy5). The FRET events are highlighted in gray, and photobleaching of the Cy3 donor dye is indicated by the arrow.

Supplementary Figure 9

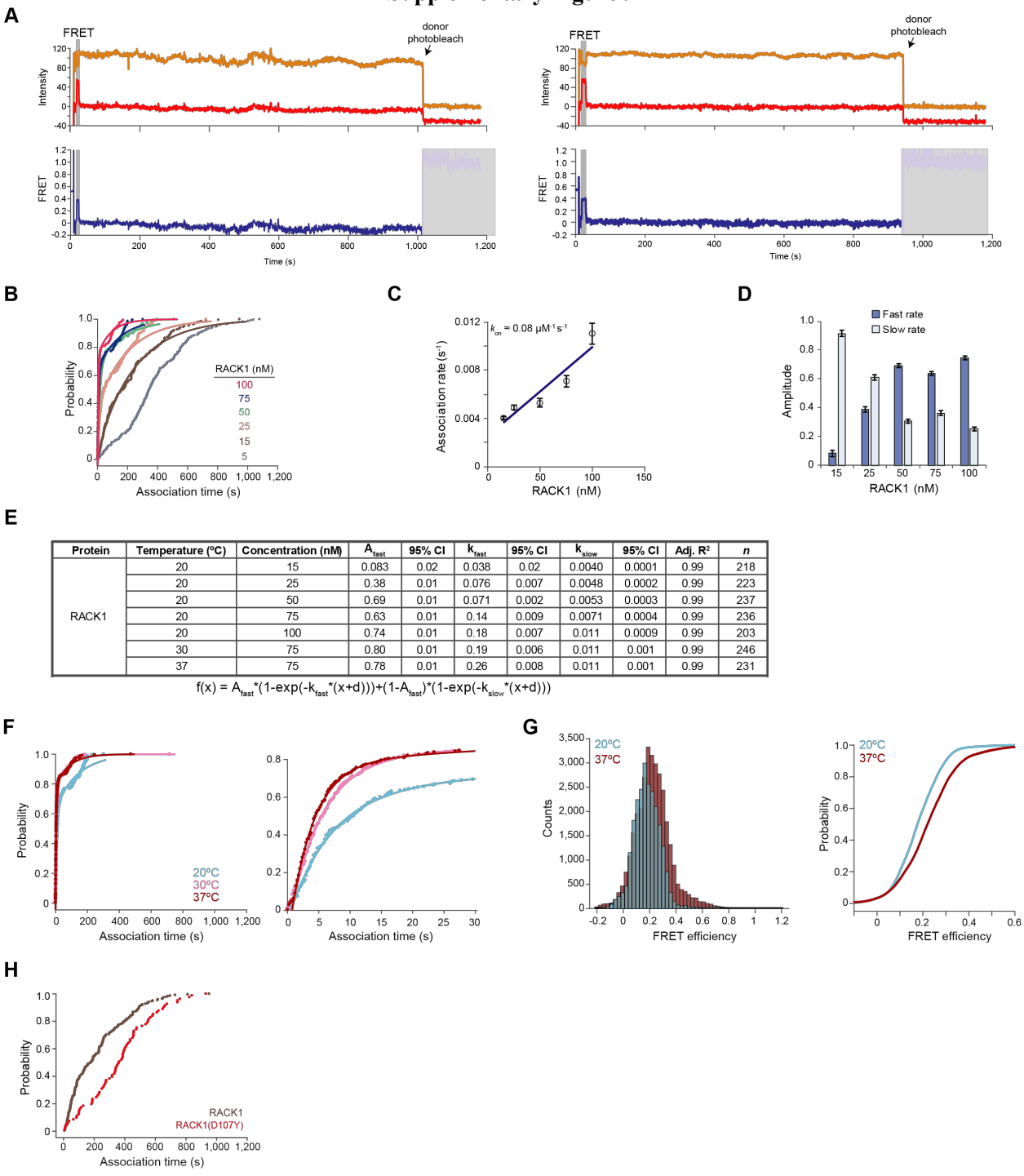

E

Protein	Temperature (ºC)	Concentration (nM)	A_{fast}	95% CI	k_{fast}	95% CI	k_{slow}	95% CI	Adj. R^2	*n*
RACK1	20	15	0.083	0.02	0.038	0.02	0.0040	0.0001	0.99	218
	20	25	0.38	0.01	0.076	0.007	0.0048	0.0002	0.99	223
	20	50	0.69	0.01	0.071	0.002	0.0053	0.0003	0.99	237
	20	75	0.63	0.01	0.14	0.009	0.0071	0.0004	0.99	236
	20	100	0.74	0.01	0.18	0.007	0.011	0.0009	0.99	203
	30	75	0.80	0.01	0.19	0.006	0.011	0.001	0.99	246
	37	75	0.78	0.01	0.26	0.008	0.011	0.001	0.99	231

$f(x) = A_{fast}*(1-\exp(-k_{fast}*(x+d)))+(1-A_{fast})*(1-\exp(-k_{slow}*(x+d)))$

Supplementary Figure 9 (related to Figure 4). Real-time monitoring of RACK1 association to single ribosomes by smFRET in ZMWs.

A. Example single-molecule fluorescence traces that captured FRET between RACK1 labeled with Cy5 and the immobilized 40S-HCV IRES(C44-Cy3.5) complex. The FRET events are highlighted in gray, and photobleaching of the Cy3.5 donor dye is indicated by the arrow.

B. Cumulative distribution plot of observed RACK1 association times from 0 to 1,200 seconds. The labels indicate RACK1-ybbR-Cy5 concentration (nM), and the lines represent fits to double-exponential functions.

C. Plot of observed RACK1 association rates (k_{obs}) of the slow phase at the indicated concentrations. Error bars represent the 95% confidence interval for each value. The line represents a fit to a linear function, with equation y = 0.00008x + 0.0025 and R^2 = 0.8889, which yielded the indicated association rate (k_{on}) for the slow phase.

D. Plot of the calculated amplitudes for the fast and slow phases yielded from fits of the indicated datasets to double-exponential functions.

E. Table of parameters yielded from fitting the indicated experiments to double-exponential functions.

F. Cumulative distribution plots of observed RACK1 association times from 0 to 1,200 (left) and 0 to 30 (right) seconds. RACK1-ybbR-Cy5 was delivered at 75 nM at the indicated temperatures. The lines represent fits to double-exponential functions.

G. Histogram (left) and cumulative distribution plots of observed FRET efficiencies between the HCV IRES-Cy3.5 (donor) and RACK1-ybbR-Cy5 (acceptor) upon RACK1 binding to the immobilized ΔRACK1 40S-IRES complex at the indicated temperatures.

H. Cumulative distribution plot of observed RACK1(D107Y) association times from 0 to 1,200 seconds after delivery at 15 nM. We replotted 15 nM RACK1-ybbR-Cy5 data from panel a here as a comparison.

Supplementary Figure 10

A

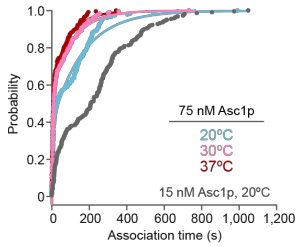

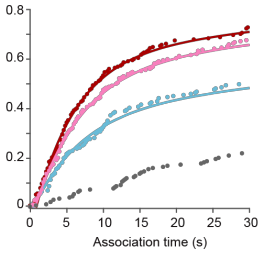

B

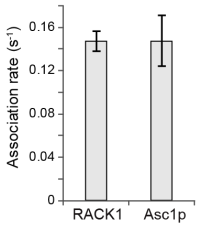

C

Protein	Temperature (ºC)	Concentration (nM)	A_{fast}	95% CI	k_{fast}	95% CI	k_{slow}	95% CI	Adj. R^2	*n*
Asc1p	20	75	0.38	0.02	0.14	0.02	0.0060	0.0003	0.98	238
	30	75	0.55	0.009	0.15	0.005	0.0091	0.0003	0.99	234
	37	75	0.60	0.01	0.17	0.008	0.011	0.0005	0.99	227

$f(x) = A_{fast}*(1-exp(-k_{fast}*(x+d)))+(1-A_{fast})*(1-exp(-k_{slow}*(x+d)))$

D

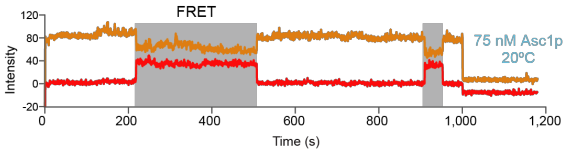

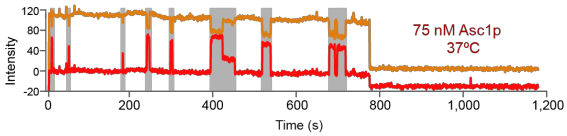

E

Asc1p (75 nM)	A	95% CI	k	95% CI	Adj. R^2	n
20ºC	0.99	0.01	0.0049	0.0001	0.99	158
30ºC	1.0	0.003	0.0067	0.00006	0.99	299
37ºC	1.0	0.005	0.011	0.0001	0.99	484

$f(x) = A*(1-exp(-k*(x+d)))$

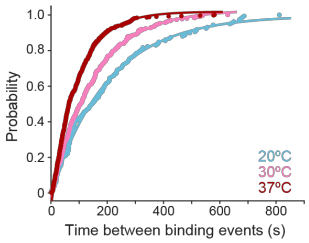

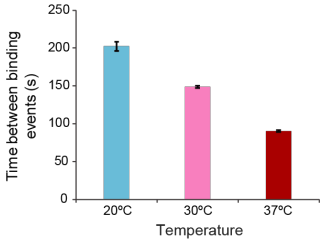

Supplementary Figure 10 (related to Figure 4). Dynamic association of *S. cerevisiae* Asc1p with 40S human ribosomal subunits measured by real-time smFRET in ZMWs.

A. Cumulative distribution plots of observed Asc1p association times from 0 to 1,200 (left) and 0 to 30 (right) seconds. Asc1p-ybbR-Cy5 was delivered at 75 nM at the indicated temperatures, as well as at 15 nM at 20˚C. The lines represent fits to double-exponential functions.

B. Plot of observed association rates (k_{obs}) for the fast phase upon delivery of 75 nM Asc1p-ybbR-Cy5 or RACK1-ybbR-Cy5 at 20˚C. Error bars represent the 95% confidence interval for each value.

C. Table of parameters yielded from fitting the indicated experiments to double-exponential functions.

D. Representative single-molecule fluorescence traces for Asc1p-ybbR-Cy5 binding to a single ΔRACK1 40S:IRES-Cy3.5 complex indicated by Cy3.5-Cy5 FRET, highlighted in gray. Single 40S-IRES complexes were identified via a single-step photobleaching event in the Cy3.5 donor signal, indicated by the arrow.

E. The time between two Asc1p binding events on a single 40S-IRES complex was measured upon its delivery at 75 nM at the indicated temperatures. The table (top) contains the parameters from fits to single-exponential functions, with *n* representing the number of binding events that were analyzed. The cumulative distribution plot (bottom left) displays the observed time between Asc1p binding events on a single 40S-IRES complex and the lines represent the fits to single-exponential functions. The bar plot (bottom right) displays the calculated times between Asc1p binding events for the indicated experiments yielded from the fits to single-exponential functions, with error bars representing the 95% confidence interval for each value.

Supplementary Figure 11

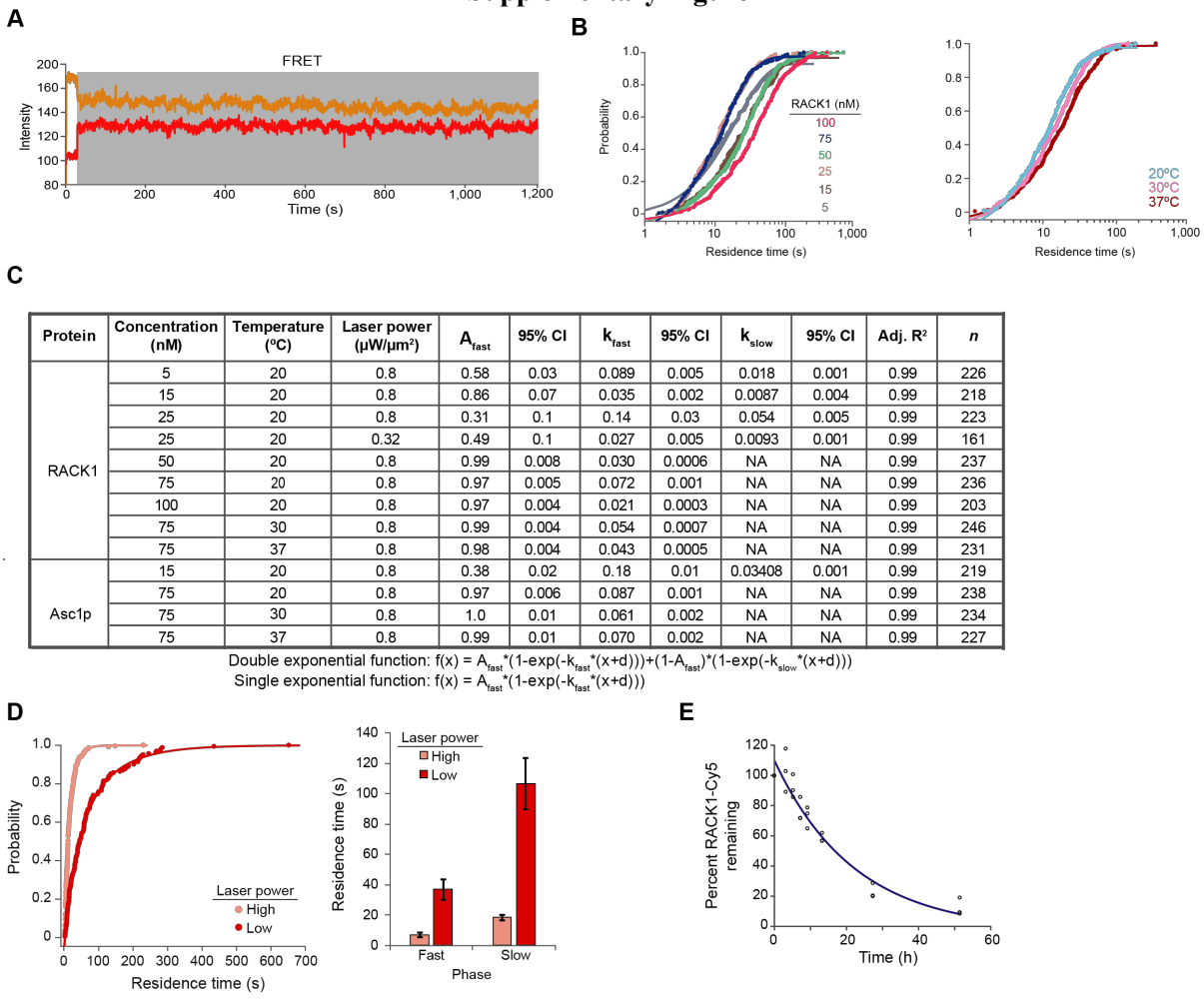

C

Protein	Concentration (nM)	Temperature (°C)	Laser power (μW/μm²)	A_{fast}	95% CI	k_{fast}	95% CI	k_{slow}	95% CI	Adj. R^2	*n*
RACK1	5	20	0.8	0.58	0.03	0.089	0.005	0.018	0.001	0.99	226
	15	20	0.8	0.86	0.07	0.035	0.002	0.0087	0.004	0.99	218
	25	20	0.8	0.31	0.1	0.14	0.03	0.054	0.005	0.99	223
	25	20	0.32	0.49	0.1	0.027	0.005	0.0093	0.001	0.99	161
	50	20	0.8	0.99	0.008	0.030	0.0006	NA	NA	0.99	237
	75	20	0.8	0.97	0.005	0.072	0.001	NA	NA	0.99	236
	100	20	0.8	0.97	0.004	0.021	0.0003	NA	NA	0.99	203
	75	30	0.8	0.99	0.004	0.054	0.0007	NA	NA	0.99	246
	75	37	0.8	0.98	0.004	0.043	0.0005	NA	NA	0.99	231
Asc1p	15	20	0.8	0.38	0.02	0.18	0.01	0.03408	0.001	0.99	219
	75	20	0.8	0.97	0.006	0.087	0.001	NA	NA	0.99	238
	75	30	0.8	1.0	0.01	0.061	0.002	NA	NA	0.99	234
	75	37	0.8	0.99	0.01	0.070	0.002	NA	NA	0.99	227

Double exponential function: $f(x) = A_{fast}*(1-\exp(-k_{fast}*(x+d)))+(1-A_{fast})*(1-\exp(-k_{slow}*(x+d)))$

Single exponential function: $f(x) = A_{fast}*(1-\exp(-k_{fast}*(x+d)))$

Supplementary Figure 11 (related to Figure 4). RACK1 dissociation measurement by smFRET in ZMWs is limited by photobleaching of the dyes.

A. A single-molecule fluorescence trace (prior to background correction) for RACK1-ybbR-Cy5 binding to a single ΔRACK1 40S:IRES-Cy3.5 complex indicated by Cy3.5-Cy5 FRET, highlighted in grey. While rare due to the limited lifetime of the Cy5 dye, we observed RACK1 binding events that lasted greater than 10 minutes.

B. Cumulative distribution plots of observed RACK1 residence times at the indicated concentrations (left) and temperatures (right, delivery at 75 nM). The lines represent fits to single- or double-exponential functions, as indicated in panel c.

C. Table of parameters yielded from fitting the indicated experiments to single- or double-exponential functions. "NA" indicates the respective parameters that were not calculated since these experiments were best fit by single-exponential functions. The respective equation is listed below the table.

D. Cumulative distribution (left) and column (right) plot of observed residence times for RACK1 after delivery at 15 nM using low (0.32 μW/ μm^2) or high (0.8 μW/ μm^2) laser power. Error bars represent the 95% confidence interval for each value.

E. Native gel electrophoresis analysis of 40S-RACK1-ybbR-Cy5 following competition after the indicated times with recombinant unlabeled RACK1-ybbR at 20-fold excess. Each circle on the graph represents the fluorescence intensity remaining relative to the 0.08 h time point from each replicate, which were used to generate the plot in Figure 5h. The line represents the fit to an exponential function.